Interface Disorder in Large Single- and Multi-Shell Upconverting Nanocrystals.

Damien Hudry,[1] Radian Popescu,[2] Dmitry Busko,[1] Maria Diaz-Lopez,[3] Milinda Abeykoon,[4]

Pierre Bordet,[3] Dagmar Gerthsen,[2]

Ian Howard,[1,5] and Bryce S. Richards[1,5]

1 Institute of Microstructure Technology, Karlsruhe Institute of Technology, Hermann-von-Helmholtz-Platz 1, D-76344 Eggenstein-Leopoldshafen, Germany.

2 Laboratory of Electron Microscopy, Karlsruhe Institute of Technology, Engesserstrasse 7, D-76131 Karlsruhe, Germany.

3 Université Grenoble Alpes, CNRS, Institut Néel, 38000 Grenoble, France.

4 Photon Science Division, National Synchrotron Light Source II, Brookhaven National Laboratory, Upton, New York 11973, United States.

5 Light Technology Institute, Karlsruhe Institute of Technology, Engesserstrasse 13, D-76131 Karlsruhe, Germany.

Supporting Information

Content

1. Chemicals.

Gadolinium acetate hydrate ($Gd(OOCCH_3)_3.xH_2O$, 99.9 %), ytterbium acetate hydrate ($Yb(OOCCH_3)_3.xH_2O$, 99.9 %), erbium acetate hydrate ($Er(OOCCH_3)_3.xH_2O$, 99.9 %), yttrium acetate hydrate ($Y(OAc)_3.xH_2O$, 99.9 %), oleic acid (OA, technical grade, 90%), octadecene (ODE, technical 90%), sodium hydroxide (NaOH, anhydrous, 98%), ammonium fluoride (NH_4F, 99.99%), sodium trifluoroacetate (98%) anhydrous methanol (MeOH), absolute ethanol (EtOH), and toluene ($C_6H_5CH_3$) were purchased from Sigma Aldrich and were used without further purification. Oleylamine (OAm) was purchased from Acros Organics (C18-content 80-90%) and used without further purification. Note that sodium hydroxide, ammonium fluoride, anhydrous methanol, OA, ODE, and OAm are stored under inert conditions in a glovebox under dry nitrogen (O_2 < 1 ppm, H_2O < 1 ppm). Note that all given quantities for rare earth acetate precursors were corrected based on their corresponding thermogravimetric analyses.

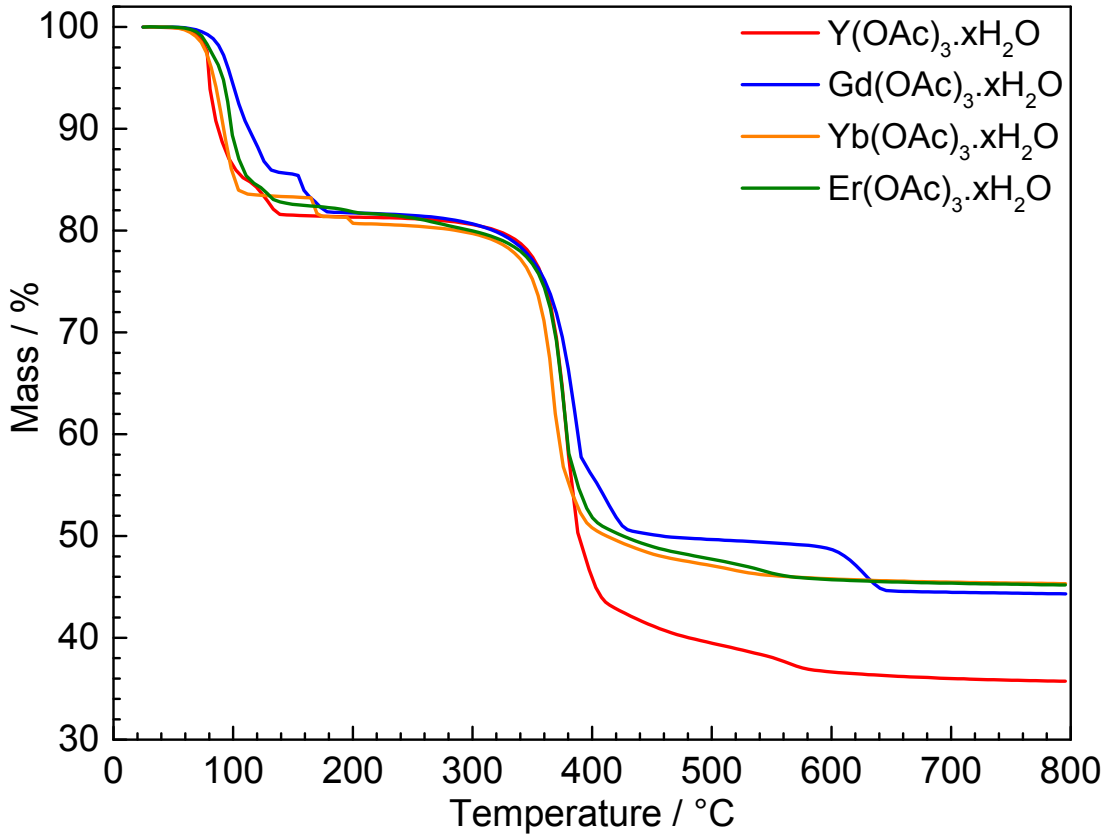

Thermogravimetric analyses of the starting rare earth acetates performed under argon with a heating rate of 10°C.min^{-1}.

2. Synthesis of rare earth trifluoroacetates.

Synthesis of $Y(OOCCF_3)_3$. $Y(OOCCF_3)_3$ was prepared by adding 10 mmol of yttrium oxide (Y_2O_3) to 6.2 mL of trifluoroacetic acid and 12.4 mL of deionized water in a 50 mL round bottom flask equipped with a reflux condenser. The stirred suspension was heated up to 90°C under air until the solid oxide was completely dissolved and a clear colorless solution was obtained (14 hours, 90°C). After cooling, the solution was filtered and the solvent evaporated with a rotary evaporator at 60°C for 90 min. The obtained wet powder was dried under vacuum at 60°C for 6 hours. The dry powder was stored under inert conditions in a glovebox under dry nitrogen (O_2 < 1 ppm, H_2O < 1 ppm). Note that the compound obtained was slightly hydrated as shown with its corresponding thermogravimetric analysis.

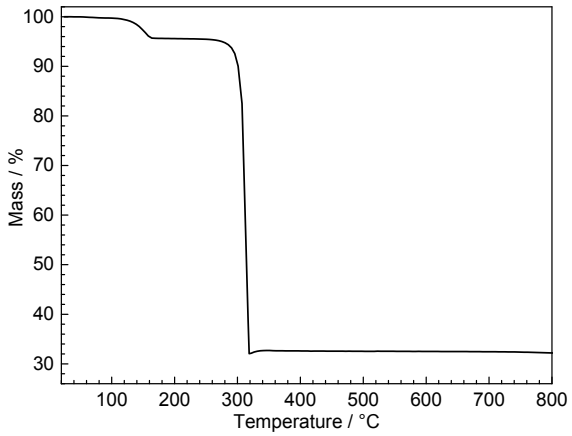

Thermogravimetric analysis of the as-prepared yttrium trifluoroacetate performed under argon with a heating rate of 10°C.min^{-1}.

Synthesis of $Gd(OOCCF_3)_3$. $Gd(OOCCF_3)_3$ was prepared by adding 10 mmol of gadolinium oxide (Gd_2O_3) to 6.2 mL of trifluoroacetic acid and 12.4 mL of deionized water in a 50 mL round bottom flask equipped with a reflux condenser. The stirred suspension was heated up to 90°C under air until the solid oxide was completely dissolved and a clear colorless solution was obtained (60 min, 90°C). After cooling, the solvent was evaporated with a rotary evaporator at 60°C for 60 min. The obtained wet powder was dried under vacuum at 60°C for 17 hours. The dry powder was stored under inert conditions in a glovebox under dry nitrogen (O_2 < 1 ppm, H_2O < 1 ppm). Note that the compound obtained was hydrated as shown with its corresponding thermogravimetric analysis.

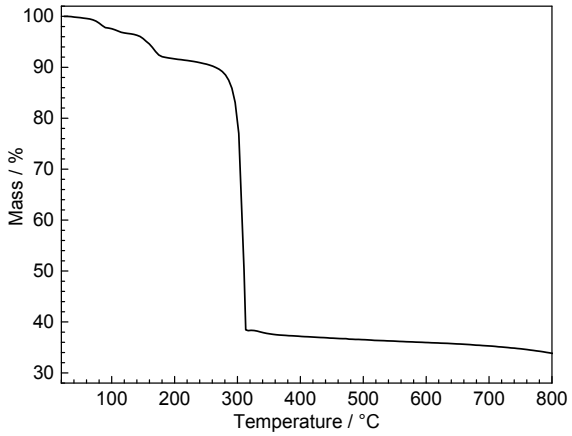

Thermogravimetric analysis of the as-prepared gadolinium trifluoroacetate performed under argon with a heating rate of 10°C.min^{-1}.

3. Synthesis of core upconverting nanocrystals.

Synthesis of β-NaEr$_{0.8}$Yb$_{0.2}$F$_4$ core nanocrystals. β-NaEr$_{0.8}$Yb$_{0.2}$F$_4$ was synthesized by the method that was first reported by Li and Zhang.[1] The synthesis has been slightly modified compared to the experimental procedure published by Wang and co-workers.[2] The synthesis was performed using air-free techniques (Schlenk line and glovebox) under purified nitrogen (glovebox) or argon (Schlenk line).

Note that all β-NaEr$_{0.8}$Yb$_{0.2}$F$_4$ seeds utilized for the subsequent growth of single- and multi-shell upconverting nanocrystals (NCs) were obtained from one single batch synthesis as described below. This is a guarantee to properly compare the optical properties of all synthesized core, single- and multi-shell NCs.

Preparation of solution A. Er(OOCCH$_3$)$_3$ (3.3 mmol) and Yb(OOCCH$_3$)$_3$ (0.8 mmol) are introduced in a 250 mL round bottom flask together with OA (40 mL) and ODE (60 mL). The resulting mixture is heated up to 120°C (under Ar) to dissolve lanthanide acetates. The white turbid solution turns to an optically clear gold / orange solution within few minutes at 120°C. After 25 minutes, the temperature is decreased to 100°C, and the optically clear solution is purified under vacuum. The vacuum purification consists in fifteen Ar ↔ vacuum (7.5.10^{-1} to 2.0.10^{-2} mbar) cycles followed by a dynamic vacuum step (5.10^{-3} mbar) for 10 minutes. The

resulting solution (solution A) is kept under static Ar and cooled down to room temperature (25°C).

Preparation of solution B. In a dry glovebox under N_2, two methanol solutions are prepared in two 50 mL centrifuge tubes. First, 10.3 mmol of NaOH are introduced in the first 50 mL centrifuge tube with 15 mL of anhydrous MeOH. Second, 16.5 mmol of NH_4F are introduced in the second 50 mL centrifuge tube with 30 mL of anhydrous MeOH. After complete dissolution (≈ 15 min), both centrifuge tubes are removed from the glovebox. Solution B is obtained by injecting the methanol solution of NaOH into the methanol solution of NH_4F. Note that solution B is prepared just before its injection into solution A.

Synthesis of β-$NaEr_{0.8}Yb_{0.2}F_4$ core NCs. Solution B is immediately injected into solution A under Ar. The resulting solution is heated up to 50°C under Ar. The temperature is maintained for 30 minutes and then MeOH is evaporated under reduced pressure - 5.10^{-3} mbar for 30 minutes. Once MeOH is completely evaporated, the resulting solution is heated up under Ar to 300°C for 90 min. Then, the heating mantle is removed, and the flask is left to cool naturally to room temperature.

Extraction and purification of β-$NaGdF_4$:Yb:Er core NCs. The raw solution (100 mL) is split into five (5x50 mL) centrifuge tubes (≈ 20 mL of raw solution per tube). After centrifuging (3000xg, 2 min) a clear dark-brown supernatant and white-pinkish precipitate are obtained in each centrifuge tubes. For each centrifuge tube, the supernatant is discarded and the resulting white-pinkish precipitate is dispersed in toluene (2 mL) to give a clear pinkish solution. Solutions obtained from the five centrifuge tubes are combined into a single unique centrifuge tube. Nanocrystals are purified by adding 30 mL of acetone and 10 mL of absolute ethanol. The solution immediately turns white turbid. After centrifuging (3000xg, 2 min) a clear slightly yellowish supernatant and white-pinkish precipitate are obtained. The supernatant is discarded and the resulting white-pinkish precipitate is dispersed in toluene (10 mL) to give a clear pinkish solution. The purification procedure (precipitation with acetone only, centrifuging, and toluene dispersion) is repeated three times. After the final dispersion

step in toluene, the solution is centrifuge at 3000xg for 3 minutes to remove all residual insoluble.

Purified β-$NaEr_{0.8}Yb_{0.2}F_4$ core UCNCs dispersed in 10 mL toluene are stored in a tightly closed glass vial. This constitutes the unique stock solution of optically active seeds for the subsequent synthesis of single- and multi-shell upconverting architectures.

Synthesis of α-$NaYF_4$ core NCs. α-$NaYF_4$ was synthesized by the method similar to the synthesis reported by Mai et al.[3] The synthesis was performed using air-free techniques (Schlenk line and glovebox) under purified nitrogen (glovebox) or argon (Schlenk line). $Y(OOCCF_3)_3$ (4 mmol) and $Na(OOCCF_3)$ (4 mmol) are introduced in a 250 mL round bottom flask together with OA (12 mL), OAm (12 mL), and ODE (24 mL). The resulting mixture is heated up to 120°C (under Ar) to dissolve trifluoroacetates. The white turbid solution turns to an optically clear yellowish solution within few minutes at 120°C. After 20 minutes, the temperature is decreased to 100°C, and the optically clear solution is purified under vacuum. The vacuum purification consists in five Ar ↔ vacuum ($3.0.10^{-2}$ mbar) cycles followed by a dynamic vacuum step ($1.5.10^{-3}$ mbar) for 10 minutes. The resulting solution is heated up under Ar to 290°C for 30 min. Then, the heating mantle is removed, and the flask is left to cool naturally to room temperature. The extraction and purification procedure is the same as for β-$NaEr_{0.8}Yb_{0.2}F_4$ core NCs. The formation of the cubic phase was checked by x-ray powder diffraction. After the last extraction step, purified α-$NaYF_4$ NCs are dried under Ar and grinded to give a white powder. This constitutes the unique source of sacrificial α-seeds for the subsequent synthesis of upconverting architectures.

4. Synthesis of single-shell upconverting nanocrystals.

Synthesis of β-$NaEr_{0.8}Yb_{0.2}F_4$/$NaYF_4$ CS_1 NCs, method I. β-$NaEr_{0.8}Yb_{0.2}F_4$:Yb:Er|$NaYF_4$ NCs were synthesized by the controlled hot injection method at 310°C.

Shell precursor solution A. The shell precursor solution A is prepared by introducing $Y(OOCCF_3)_3$ (1.16 mmol) into a 50 mL round bottom flask together with OA (6 mL) and ODE

(6 mL). The resulting mixture is heated up to 120°C (under Ar) to dissolve the trifluoroacetate. The white turbid solution turns to an optically clear and slightly yellowish solution within few minutes at 120°C. After 15 minutes, the temperature is decreased to 100°C, and the optically clear solution is purified under vacuum (same vacuum purification as for α-$NaYF_4$ core NCs). The resulting solution is transferred into a dry glovebox under N_2 where it can be safely stored. **The final Y concentration is 0.1 mmol/mL.**

Shell precursor solution B. The shell precursor solution B is prepared by introducing $NaOOCCF_3$ (1.16 mmol) into a 50 mL round bottom flask together with OA (6 mL) and ODE (6 mL). The resulting mixture is heated up to 120°C (under Ar) to dissolve the trifluoroacetate. The white turbid solution turns to an optically clear colorless solution within few minutes at 120°C. After 20 minutes, the temperature is decreased to 100°C, and the optically clear solution is purified under vacuum (same vacuum purification as for α-$NaYF_4$ core NCs). The resulting solution is transferred into a dry glovebox under N_2 where it can be safely stored. **The final Na concentration is 0.1 mmol/mL.**

Seeds solution. The seeds solution is prepared by introducing 1 mL of β-$NaEr_{0.8}Yb_{0.2}F_4$ core NCs stock solution into a 50 mL round bottom flask together with OA (4 mL) and ODE (6 mL). The resulting mixture is heated up to 100°C (under Ar) and purified under vacuum. The vacuum purification consists in five Ar $\leftrightarrow$ vacuum ($1.5.10^{-2}$ mbar) cycles.

Synthesis of β-$NaEr_{0.8}Yb_{0.2}F_4|NaYF_4$ CS_l NCs. The purified seeds solution is heated up under Ar to 310°C. Then, 4 mL of shell precursor solution A and 4 mL of shell precursor solution B are mixed under inert atmosphere (glovebox) and introduced under Ar in a 10 mL disposable syringe equipped with a stainless steel needle, which is then fixed on a syringe pump. Then the combined shell precursor solution is slowly injected (300 μL/min) into the seeds solution. After injection, the temperature is maintained at 310°C for aging. After 60 minutes, the heating mantle is removed, and the flask is left to cool naturally to room

temperature. CS_I NCs are extracted and purified with a similar method as described for β-$NaEr_{0.8}Yb_{0.2}F_4$ core NCs and stored in 2 mL toluene.

Synthesis of β-$NaEr_{0.8}Yb_{0.2}F_4$/$NaYF_4$ CS_{II} NCs, method II. β-$NaEr_{0.8}Yb_{0.2}F_4$:Yb:Er|$NaYF_4$ NCs were synthesized by the controlled hot injection method at 310°C.

Shell precursor solution. The shell precursor solution is prepared by introducing $Y(OOCCH_3)_3$ (0.4 mmol) into a 50 mL round bottom flask together with OA (4 mL) and ODE (6 mL). The resulting mixture is heated up to 140°C (under Ar) to dissolve the acetate. The white turbid solution turns to an optically clear and slightly yellowish solution within few minutes at 140°C. After 20 minutes, the temperature is decreased to 100°C, and the optically clear solution is purified under vacuum (same vacuum purification as for α-$NaYF_4$ core NCs). The resulting solution is cooled down to room temperature (25°C). 1 mmol of NaOH and 1.6 mmol of NH_4F previously dissolved in anhydrous MeOH (glovebox) (2 mL and 4 mL, respectively) are mixed under Ar and quickly injected into the previous solution. The resulting solution is heated up to 50°C under Ar. The temperature is maintained for 30 minutes and then MeOH is evaporated under reduced pressure - 5.10^{-3} mbar for 30 minutes. The obtained solution is stored into a 10 mL disposable syringe equipped with a stainless steel needle and kept under static Ar.

Seeds solution. The seeds solution is prepared by introducing 1 mL of β-$NaEr_{0.8}Yb_{0.2}F_4$ core NCs stock solution into a 50 mL round bottom flask together with OA (4 mL) and ODE (6 mL). The resulting mixture is heated up to 100°C (under Ar) and purified under vacuum. The vacuum purification consists in five Ar ↔ vacuum ($1.5.10^{-2}$ mbar) cycles.

Synthesis of β-$NaEr_{0.8}Yb_{0.2}F_4$|$NaYF_4$ CS_{II} NCs. The purified seeds solution is heated up under Ar to 310°C. Then, the shell precursor solution is slowly injected (300 μL/min) into the seeds solution. After injection, the temperature is maintained at 310°C for aging. After 60 minutes, the heating mantle is removed, and the flask is left to cool naturally to room temperature. CS_{II} NCs are extracted and purified with a similar method as described for β-$NaEr_{0.8}Yb_{0.2}F_4$ core NCs and stored in 2 mL toluene.

Synthesis of β-NaEr$_{0.8}$Yb$_{0.2}$F$_4$/NaYF$_4$ CS$_{III}$ NCs, method III. β-NaEr$_{0.8}$Yb$_{0.2}$F$_4$:Yb:Er|NaYF$_4$ NCs were synthesized by the controlled hot injection method at 310°C.

Shell precursor solution. The shell precursor solution is prepared by introducing 80 mg of α-NaYF$_4$ into a 50 mL round bottom flask together with OA (4 mL) and ODE (6 mL). The resulting mixture is heated up to 120°C (under Ar). After 15 minutes, the temperature is decreased to 100°C, and the solution is purified under vacuum (same vacuum purification as for α-NaYF$_4$ core NCs). The resulting solution is stored into a 10 mL disposable syringe equipped with a stainless steel needle and kept under static Ar.

Seeds solution. The seeds solution is prepared by introducing 1 mL of β-NaEr$_{0.8}$Yb$_{0.2}$F$_4$ core NCs stock solution into a 50 mL round bottom flask together with OA (4 mL) and ODE (6 mL). The resulting mixture is heated up to 100°C (under Ar) and purified under vacuum. The vacuum purification consists in five Ar ↔ vacuum (1.5.10^{-2} mbar) cycles.

Synthesis of β-NaEr$_{0.8}$Yb$_{0.2}$F$_4$|NaYF$_4$ CS$_{III}$ NCs. The purified seeds solution is heated up under Ar to 310°C. Then, the shell precursor solution is slowly injected (300 μL/min) into the seeds solution. After injection, the temperature is maintained at 310°C for aging. After 60 minutes, the heating mantle is removed, and the flask is left to cool naturally to room temperature. CS$_{III}$ NCs are extracted and purified with a similar method as described for β-NaEr$_{0.8}$Yb$_{0.2}$F$_4$ core NCs and stored in 2 mL toluene.

5. Synthesis of multi-shell upconverting nanocrystals.

Synthesis of β-NaEr$_{0.8}$Yb$_{0.2}$F$_4$/NaYF$_4$/NaGdF$_4$ C2S$_I$ NCs, method I. β-NaEr$_{0.8}$Yb$_{0.2}$F$_4$|NaYF$_4$|NaGdF$_4$ (C2S$_I$) NCs were synthesized by the controlled hot injection method.

Shell precursor solution C. The shell precursor solution C is prepared by introducing Gd(OOCCF$_3$)$_3$ (1 mmol) into a 50 mL round bottom flask together with OA (5 mL) and ODE (5 mL). The resulting mixture is heated up to 120°C (under Ar) to dissolve the

trifluoroacetate. The white turbid solution turns to an optically clear and slightly yellowish solution within few minutes at 120°C. After 15 minutes, the temperature is decreased to 100°C, and the optically clear solution is purified under vacuum (same vacuum purification as for α-$NaYF_4$ core NCs). The resulting solution is transferred into a dry glovebox under N_2 where it can be safely stored. **The final Gd concentration is 0.1 mmol/mL.**

Shell precursor solution D. The shell precursor solution D is prepared by introducing $NaOOCCF_3$ (1 mmol) into a 50 mL round bottom flask together with OA (5 mL) and ODE (5 mL). The resulting mixture is heated up to 120°C (under Ar) to dissolve the trifluoroacetate. The white turbid solution turns to an optically clear colorless solution within few minutes at 120°C. After 20 minutes, the temperature is decreased to 100°C, and the optically clear solution is purified under vacuum (same vacuum purification as for α-$NaYF_4$ core NCs). The resulting solution is transferred into a dry glovebox under N_2 where it can be safely stored. **The final Na concentration is 0.1 mmol/mL**.

Seeds solution. The seeds solution is prepared by introducing 700 μL of β-$NaEr_{0.8}Yb_{0.2}F_4|NaYF_4$ stock solution into a 50 mL round bottom flask together with OA (4 mL) and ODE (6 mL). The resulting mixture is heated up to 100°C (under Ar) and purified under vacuum. The vacuum purification consists in five Ar $\leftrightarrow$ vacuum ($1.5.10^{-2}$ mbar) cycles.

Synthesis of β-$NaEr_{0.8}Yb_{0.2}F_4|NaYF_4|NaGdF_4$ $C2S_l$ NCs. The purified seeds solution is heated up under Ar to 310°C. Then, 3 mL of shell precursor solution C and 3 mL of shell precursor solution D are mixed under inert atmosphere (glovebox) and introduced under Ar in a 10 mL disposable syringe equipped with a stainless steel needle, which is then fixed on a syringe pump. Then the combined shell precursor solution is slowly injected (300 μL/min) into the seeds solution. After injection, the temperature is maintained at 310°C for aging. After 60 minutes, the heating mantle is removed, and the flask is left to cool naturally to room temperature. $C2S_l$ NCs are extracted and purified with a similar method as described for β-$NaEr_{0.8}Yb_{0.2}F_4$ core NCs and stored in 1 mL toluene.

Synthesis of β-$NaEr_{0.8}Yb_{0.2}F_4$\|$NaYF_4$\|$NaGdF_4$\|$NaYF_4$ C3S$_I$ NCs, method I. β-$NaEr_{0.8}Yb_{0.2}F_4$\|$NaYF_4$\|$NaGdF_4$\|$NaYF_4$ (C3S$_I$) NCs were synthesized by the controlled hot injection method. $NaEr_{0.8}Yb_{0.2}F_4$ NCs from the stock solution were used as the starting seeds. CS$_I$ ($NaEr_{0.8}Yb_{0.2}F_4$\|$NaYF_4$) NCs were synthesized exactly as described previously but the amount of seeds (C NCs) was slightly increased (1500 μL instead of 1000 μL) to limit the final size of C3S$_I$ NCs. C2S$_I$ ($NaEr_{0.8}Yb_{0.2}F_4$\|$NaYF_4$\|$NaGdF_4$) were synthesized as described previously but the amount of seeds (CS NCs) was slightly increased (1000 μL instead of 700 μL) to limit the final size of C3S$_I$ NCs.

Seeds solution. The seeds solution is prepared by introducing 1 mL of β-$NaEr_{0.8}Yb_{0.2}F_4$\|$NaYF_4$\|$NaGdF_4$ stock solution into a 50 mL round bottom flask together with OA (4 mL) and ODE (6 mL). The resulting mixture is heated up to 100°C (under Ar) and purified under vacuum. The vacuum purification consists in five Ar ↔ vacuum ($1.5.10^{-2}$ mbar) cycles.

Synthesis of β-$NaEr_{0.8}Yb_{0.2}F_4$\|$NaYF_4$\|$NaGdF_4$\|$NaYF_4$ C3S$_I$ NCs. The purified seeds solution is heated up under Ar to 310°C. Then, 2 mL of shell precursor solution A and 2 mL of shell precursor solution B (stock solutions prepared for the synthesis of β-$NaEr_{0.8}Yb_{0.2}F_4$\|$NaYF_4$, method I) are mixed under inert atmosphere (glovebox) and introduced under Ar in a 10 mL disposable syringe equipped with a stainless steel needle, which is then fixed on a syringe pump. Then the combined shell precursor solution is slowly injected (300 μL/min) into the seeds solution. After injection, the temperature is maintained at 310°C for aging. After 60 minutes, the heating mantle is removed, and the flask is left to cool naturally to room temperature. C3S$_I$ NCs are extracted and purified with a similar method as described for β-$NaEr_{0.8}Yb_{0.2}F_4$ core NCs and stored in 1 mL toluene.

6. Transmission electron microscopy (TEM) and scanning transmission electron microscopy (STEM).

Sample preparation. Transmission electron microscopy (TEM) samples were prepared (room temperature, air) by drop-casting 10 µL of diluted suspension of the NCs dispersed in toluene onto an ultrathin carbon film (2 nm) on holey carbon support film mounted on 400 µm mesh Cu grid (Ted Pella Inc.).

Instruments. The size, morphology and structure of nanoparticles were investigated by high-resolution (HR) TEM and high-angle annular dark-field (HAADF) scanning transmission electron microscopy (STEM) conducted with an aberration-corrected FEI Titan 80-300 microscope at 300 keV electron energy and a FEI Osiris ChemiSTEM microscope at 200 keV.

High-resolution transmission electron microscopy (HRTEM). HRTEM images were evaluated by calculating their two-dimensional (2D) Fourier transform (FT) patterns, which yields information on the crystal structure (lattice parameters and crystal symmetry) of single NCs. The analysis was performed by comparing the experimental 2D FT patterns and calculated diffraction patterns, where the latter were obtained by using the JEMS (Java version of the electron microscopy simulation) software.[4] The zero-order beam (ZB) is indicated in the 2D FT patterns.

7. Chemical information from transmission electron microscopy.

Chemical information was obtained by HAADF-STEM combined with energy-dispersive X-ray spectroscopy (EDXS). The experiments were carried out with a FEI Osiris ChemiSTEM microscope, which is equipped with a Bruker Quantax system (XFlash detector) for EDXS. EDX spectra are quantified with the FEI software package “TEM imaging and analysis” (TIA) version 4.7 SP3. Using TIA, element concentrations were calculated on the basis of a refined Kramers’ law model, which includes corrections for detector absorption and background subtraction. For this

purpose, standard-less quantification (theoretical sensitivity factors) without thickness correction was applied. The quantification of Na-, F-, Y-, Gd-, Yb- and Er-content from their EDX spectra (line or area scans) was performed by evaluating the intensities of the F-$K_{\alpha 1}$ line, Na-K series, Y-L series, Gd-L series, Yb-L series and Er-L series. We noted that X-ray lines of Cu (K- and L-series) from the grid, Gd-M, Er-M and Yb-M series from nanoparticles, as well as the C-$K_{\alpha 1}$ line from the amorphous carbon substrate were always present in the EDXS spectra. In addition Si-K and O-$K_{\alpha 1}$ lines result from SiO_2 contamination of the TEM specimens.

Elemental maps and average chemical composition (area scans). EDX spectra obtained by scanning rectangular areas (ensembles of particles) were acquired. Elemental maps of Na (Na-$K_{\alpha 1}$ line), F (F-$K_{\alpha 1}$ line), Y (Y-$L_{\alpha 1}$ line), Gd (Gd-$L_{\alpha 1}$ line), Yb (Yb-$L_{\alpha 1}$ line) and Er (Er-$L_{\alpha 1}$) were obtained and used to investigate the distribution of these elements in all synthesized NCs. Elemental maps were analyzed by using the ESPRIT software (version 1.9) from Bruker. The measured Na and F concentrations are a sum of their real concentration within NCs and their concentrations on the substrate under the NCs. Hence, the Na/F concentrations on the substrate were determined and subtracted from the Na/F concentrations measured from the area scans to extract real NC concentrations. For this purpose, EDXS area scans were also acquired and quantified on particle-free regions close to the investigated areas.

Local chemical composition (line scans). Concentration profiles of different elements within a single NC were obtained from EDX spectra acquired along a line through the center of the corresponding NC. The EDXS line profiles were taken with a probe diameter of 0.5 nm and a distance of about 1 nm between two measuring points along the line. In analogy to area scans, the Na and F concentrations on the substrate under the NC were determined and subtracted from the total Na/F concentrations measured within the corresponding NC. In this case, the Na/F concentrations on the substrate were calculated by linear interpolation of the Na/F concentrations measured

along the same EDXS line scan but on regions of the substrate exceeding the NC limits on both sides (left and right). Regarding the quantification of the EDX spectra of single core-shell NC, one has to keep in mind that the obtained compositions are averaged along the electron-beam direction. In other words, the whole volume along the electron trajectory contributes to the detected X-ray signal. To determine the composition of different regions of single- and multi-shell NCs, a procedure was developed and is outlined elsewhere.[5]

8. High-energy synchrotron X-ray powder diffraction (XPD).

Measurements. High-energy XPD measurements were carried out at the Pair Distribution Function (PDF, 28-ID-1) beamline at the National Synchrotron Light Source II (NSLS-II) at Brookhaven National Laboratory (USA). Measurements were performed, at room temperature, in capillary transmission geometry using a (0.5 x 0.5) mm^2 monochromatic (66.7 keV; λ = 0.18179 Å) x-ray beam. A PerkinElmer amorphous silicon area detector, mounted orthogonal to the beam path was used for data collection. Total scattering measurements were carried out using the detector at the sample-to-detector distance 204 mm. All measured samples were compacted powders sealed in kapton capillaries (internal diameter: 1 mm, wall thickness: 0.1 mm). Microcrystalline nickel powder in a kapton capillary (internal diameter: 1 mm, wall thickness: 0.1 mm) was used as a reference.

Data treatment. 2-D diffraction data were radially integrated to obtain 1-D patterns and converted to intensity versus 2θ using the software FIT2D[6] where 2θ is the angle between the incident and diffracted X-ray beams.

Rietveld and PDF refinements. The Rietveld refinements of the XPD data were performed with the FullProf Software.[7] The background was fitted with a Chebyshev polynomial and the profile shape was described using a modified Thompson-Cox-Hasting pseudo-Voigt function where instrumental profiles were determined by the refinement of a Ni standard with a high degree of crystallinity. The scale factor, lattice parameters, coherent domain size, relative

occupancies for Na, (∑Er, Yb), Y and Gd and isotropic displacement parameters (U_{iso}) were freely refined. Regarding the refinement of atomic positions, only zNa2, xF1 and yF1 were found not to lie within special positions and, since these correspond to low Z atoms scarcely contributing to the overall scattered intensity in the presence of heavier elements, all the atomic positions were fixed to their initial values during the refinement.

The line broadening in the three samples investigated could only be attributed to the limited size of the coherent domains in the three samples investigated. When refined, domain microstrain parameters converged to zero and they were consequently fixed to this value in the final refinements.

Additionally, XPD data were corrected and Fourier Transformed using the PDFGetX3[8] software with Q_{max} = 25 $Å^{-1}$ and thereby obtained PDF data were refined using the PDFgui software.[9] Structural parameters of the models are: i) the unit cell parameters; ii) the atomic coordinates; iii) isotropic atomic displacement parameters (U_{iso}); and iv) coherent length. Non-structural parameters are: i) the scale factor; ii) the correction factor for the finite instrumental resolution (Q_{damp}); iii) the low-r correlated motion peak sharpening factor ($\delta 1$); and iv) the Q-dependent peak broadening (Q_{broad}) factor. Q_{damp} is responsible for the damping of the PDF and was determined from the microcrystalline nickel reference and fixed for the refinements of NCs.

9. Supplementary figures

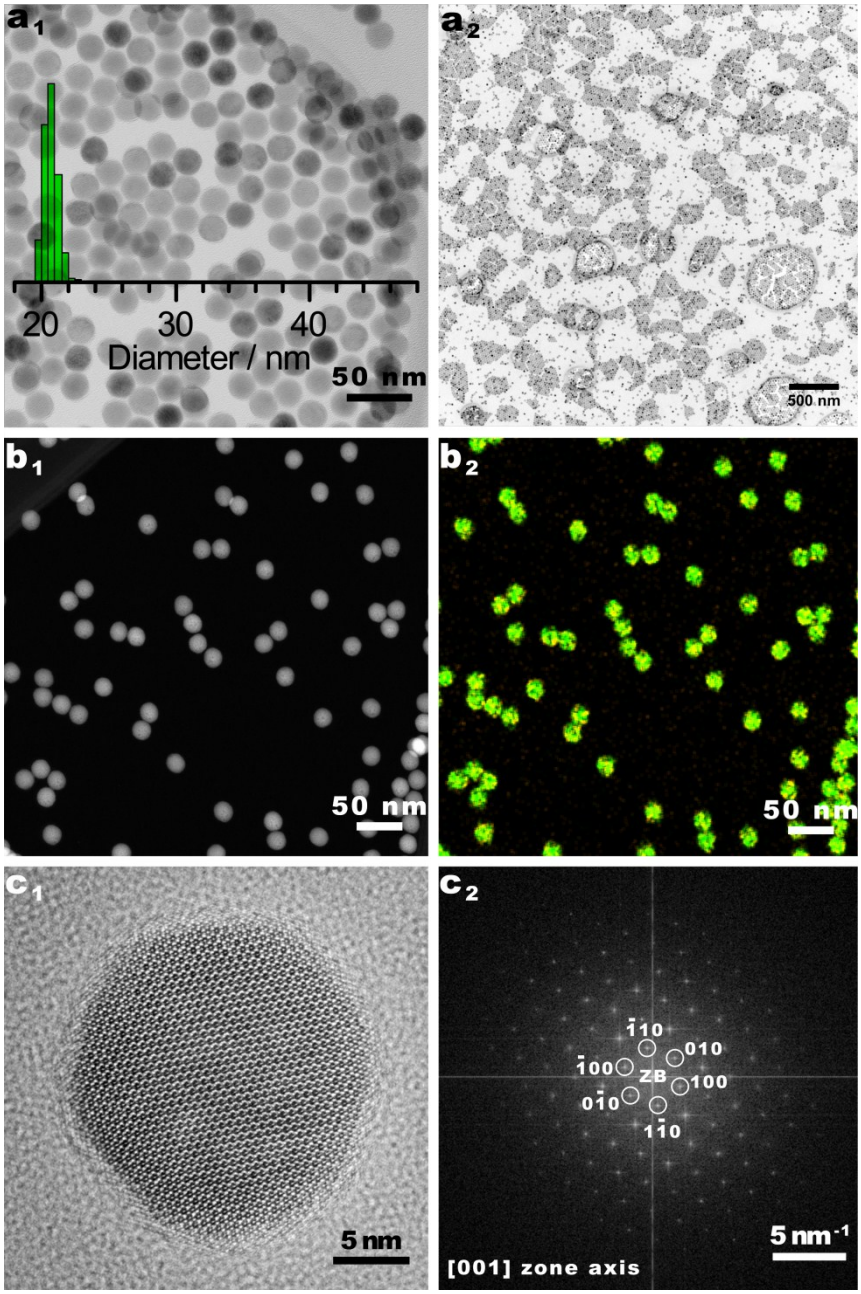

Figure S1. *(a_1-a_2) Bright-field transmission electron microscopy micrographs and overlaid size distribution histogram, (b_1) high-angle annular dark-field scanning transmission electron microscopy (HAADF-STEM) micrographs and (b_2) corresponding elemental map obtained by energy dispersive x-ray spectroscopy (EDXS), (c_1) high-resolution transmission electron microscopy micrograph with (c_2) its corresponding two-dimensional Fourier transform (FT) patterns of core $NaEr_{0.8}Yb_{0.2}F_4$ upconverting nanocrystals. Color coding used for the elemental map: Er (green), and Yb (orange). The indexing of the two-dimensional FT patterns is compatible with the hexagonal phase (β-phase, space group $P\bar{6}$, #174).*

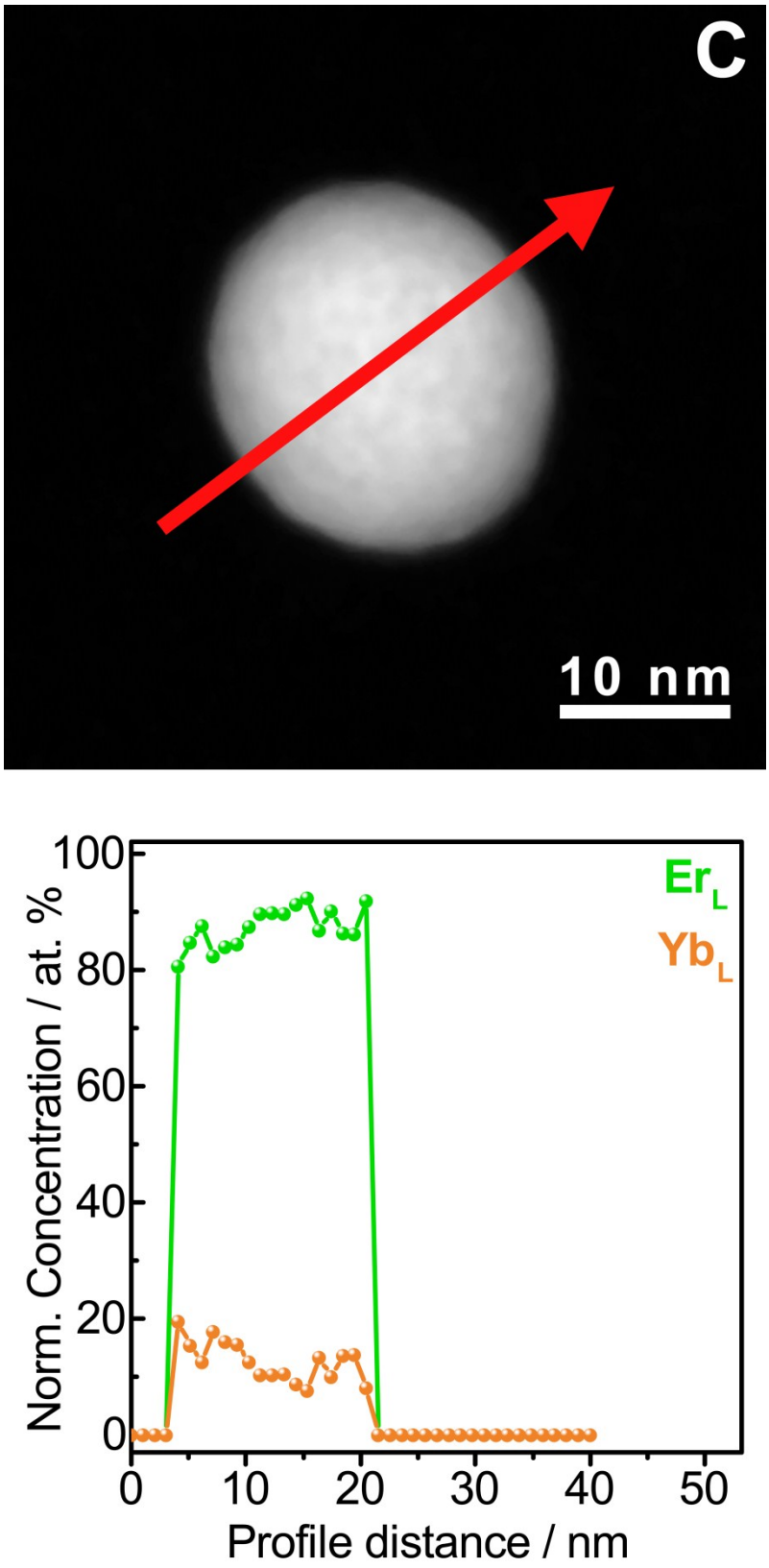

Figure S2. *High-angle annular dark-field scanning transmission electron microscopy (HAADF-STEM) micrograph with red arrow indicating the energy dispersive x-ray spectroscopy (EDXS) scan direction of individual* $NaEr_{0.8}Yb_{0.2}F_4$ / $NaYF_4$ *core upconverting nanocrystal (top), and the corresponding structure-independent concentration profiles (erbium – green; ytterbium – orange) (bottom).*

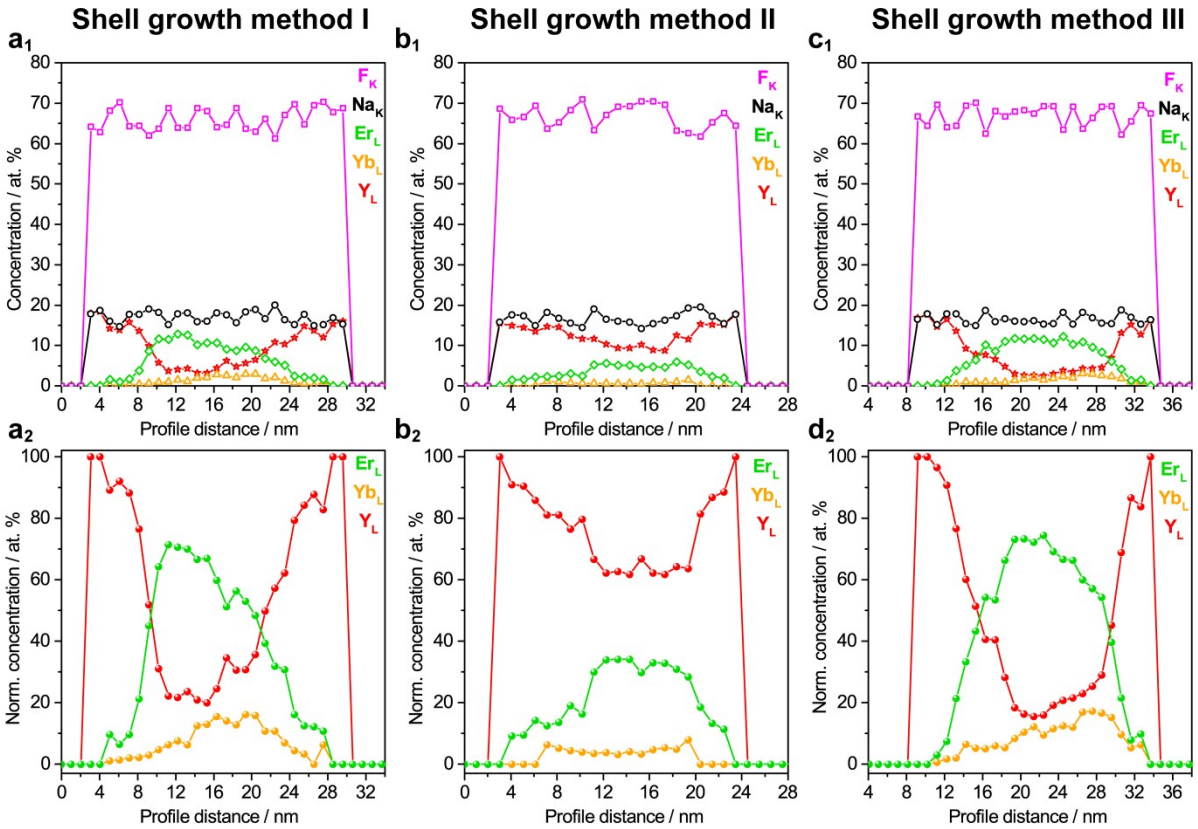

Figure S3. *(a_1-c_1) Overall and (a_2-c_2) normalized concentration profiles extracted for $NaEr_{0.8}Yb_{0.2}F_4$ /$NaYF_4$ CS nanocrystals synthesized by Methods I ($a_{1\text{-}2}$), II ($b_{1\text{-}2}$), and III ($c_{1\text{-}2}$). For each nanocrystal, normalization was performed relative to the total amount of lanthanide (erbium, ytterbium, yttrium).*

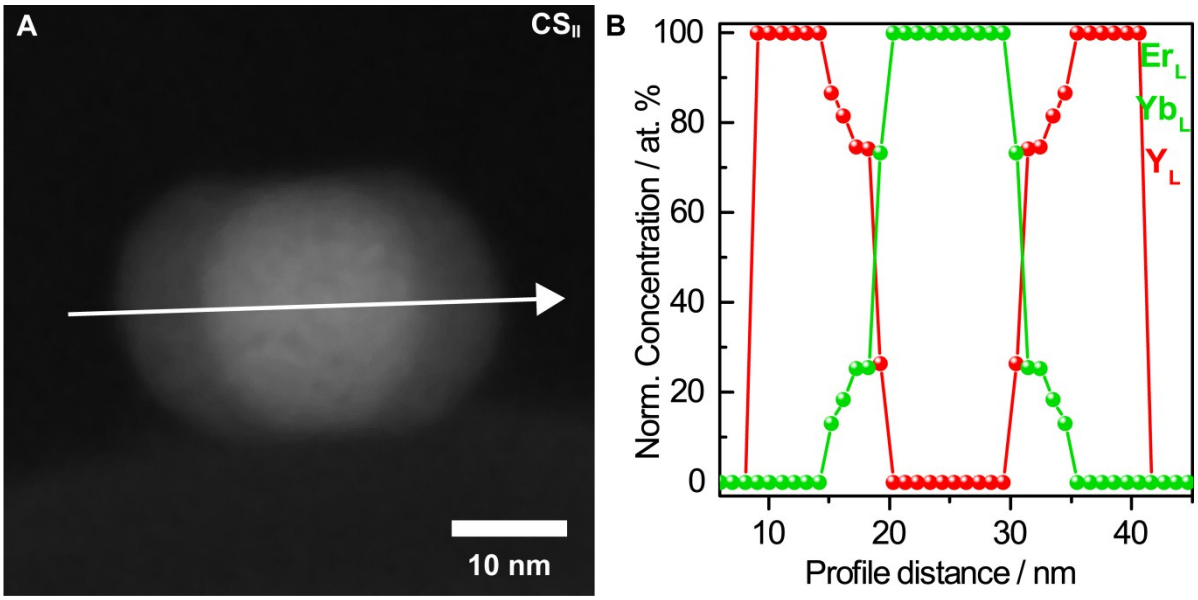

Figure S4. *(A) High-angle annular dark-field scanning transmission electron microscopy (HAADF-STEM) micrograph with white arrow indicating the energy dispersive x-ray spectroscopy (EDXS) scan directions of individual* $NaEr_{0.8}Yb_{0.2}F_4$ */* $NaYF_4$ CS_{II} *upconverting nanocrystals (NCs), and (B) the corresponding structure-independent concentration profile (erbium/ytterbium – green; yttrium – red).*

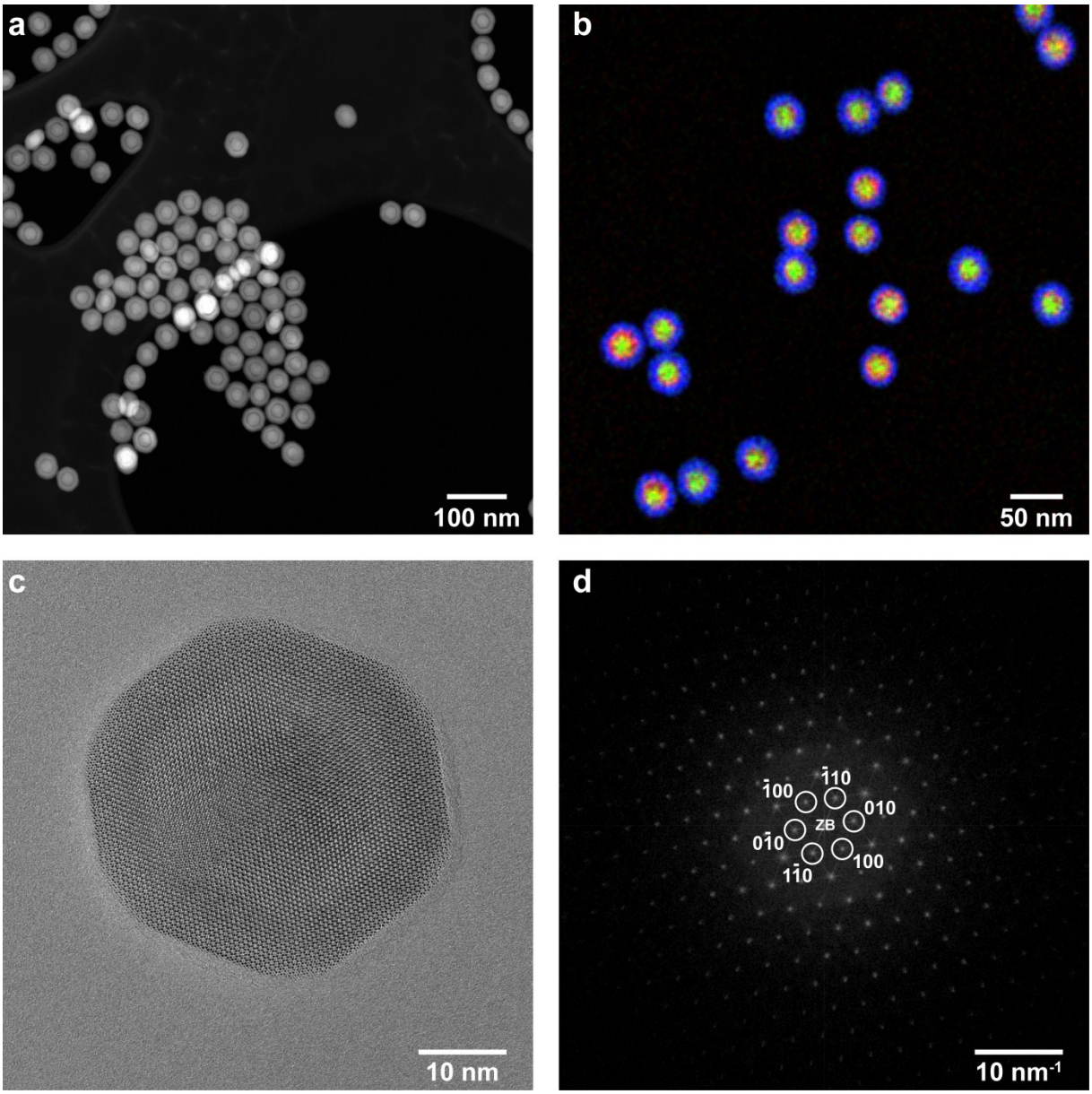

Figure S5. *Characterization of $NaEr_{0.8}Yb_{0.2}F_4$ / $NaYF_4$ / $NaGdF_4$ C2S$_I$ upconverting nanocrystals synthesized with the shell deposition Method I. a) High-angle annular dark-field scanning transmission electron microscopy (HAADF-STEM) micrograph, b) elemental map obtained by energy dispersive x-ray spectroscopy (EDXS), c) high-resolution transmission electron microscopy micrograph and d) corresponding two-dimensional Fourier transform (FT) pattern. Color coding used for the elemental map: Er (green), Yb (orange), Y (red), and Gd (blue).The indexing of the two-dimensional FT pattern is compatible with the hexagonal phase (β-phase, space group $P\bar{6}$, #174) in the [001] zone axis.*

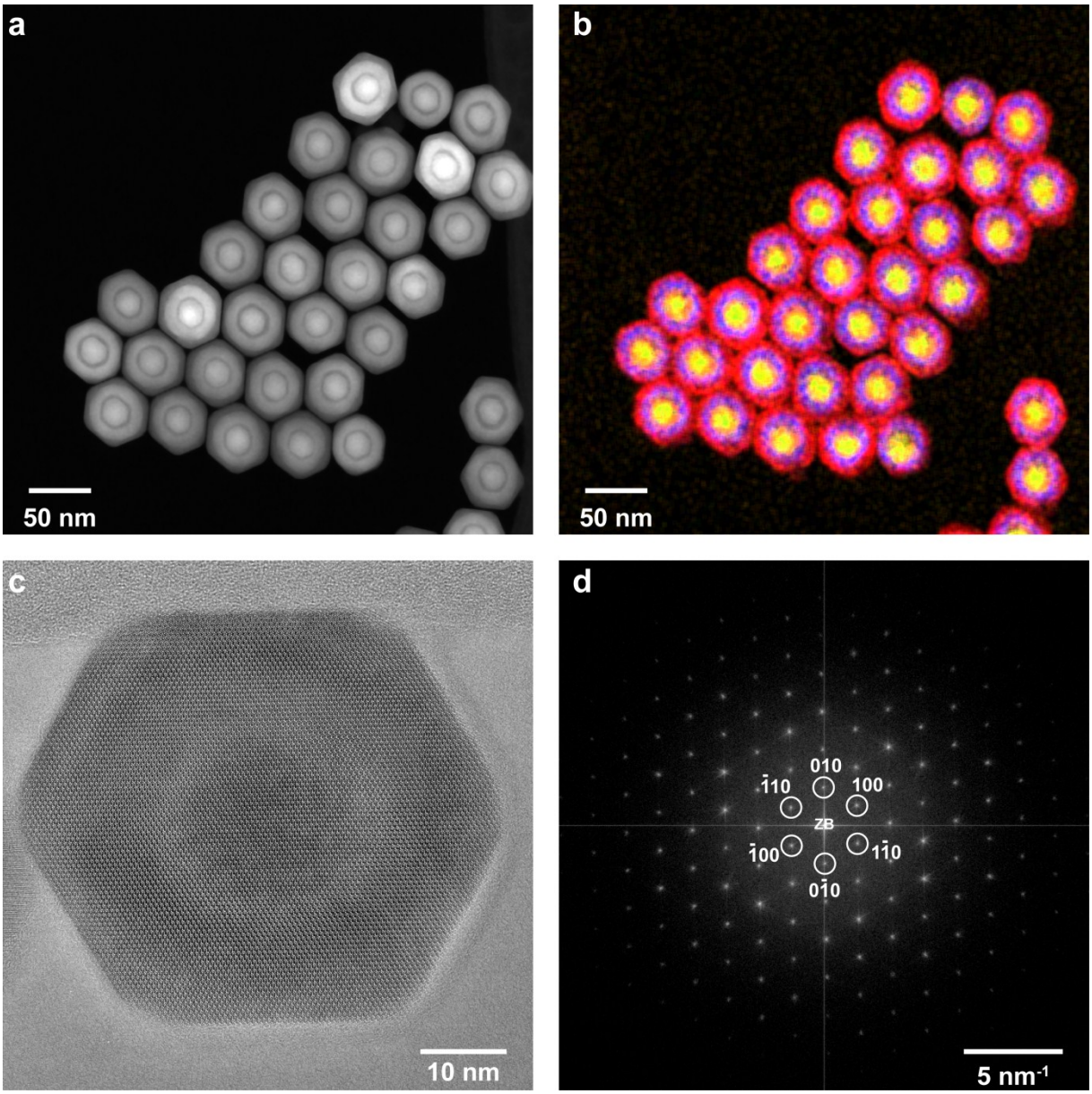

Figure S6. *Characterization of $NaEr_{0.8}Yb_{0.2}F_4$ / $NaYF_4$ / $NaGdF_4$ / $NaYF_4$ C3S$_I$ upconverting nanocrystals synthesized with the shell deposition Method I. a) High-angle annular dark-field scanning transmission electron microscopy (HAADF-STEM) micrograph, b) elemental map obtained by energy dispersive x-ray spectroscopy (EDXS), c) high-resolution transmission electron microscopy micrograph and d) corresponding two-dimensional Fourier transform (FT) pattern. Color coding used for the elemental map: Er (green), Yb (orange), Y (red), and Gd (blue).The indexing of the two-dimensional FT pattern is compatible with the hexagonal phase (β-phase, space group $P\bar{6}$, #174) in the [001] zone axis.*

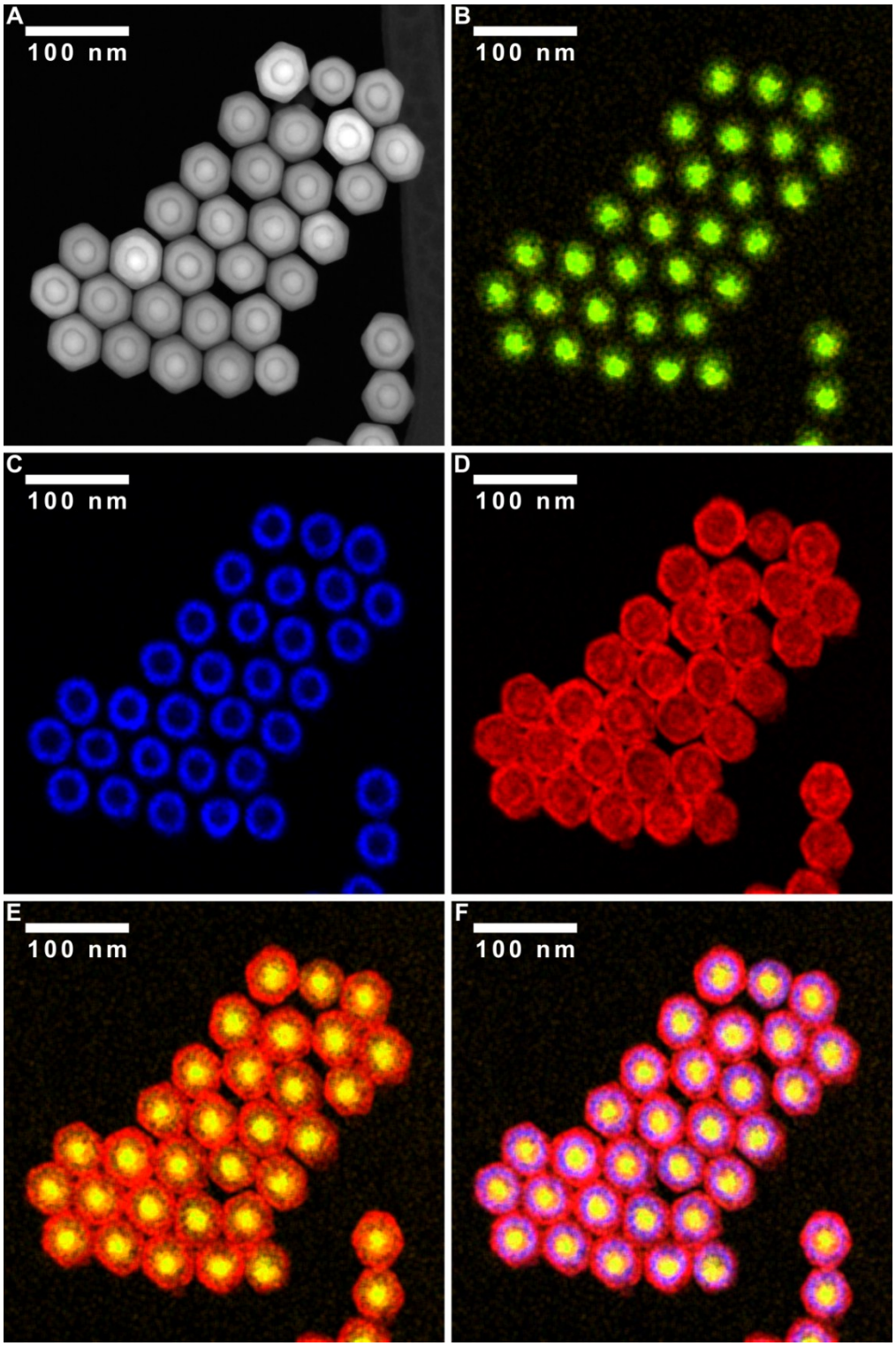

Supplement to Figure S6b. *A) High-angle annular dark-field scanning transmission electron microscopy (HAADF-STEM) micrograph and B-F) corresponding elemental maps obtained by energy dispersive x-ray spectroscopy (EDXS) of* $NaEr_{0.8}Yb_{0.2}F_4$ / $NaYF_4$ / $NaGdF_4$ / $NaYF_4$ *C3S upconverting nanocrystals synthesized with the shell deposition Method I. B) Er / Yb map, C) Gd map, D) Y map, E) combined Er / Yb, Y maps, and F) combined Er / Yb, Y, Gd maps. Color coding utilized for elemental maps: Er and Yb (green), Gd (blue), and Y (red)*

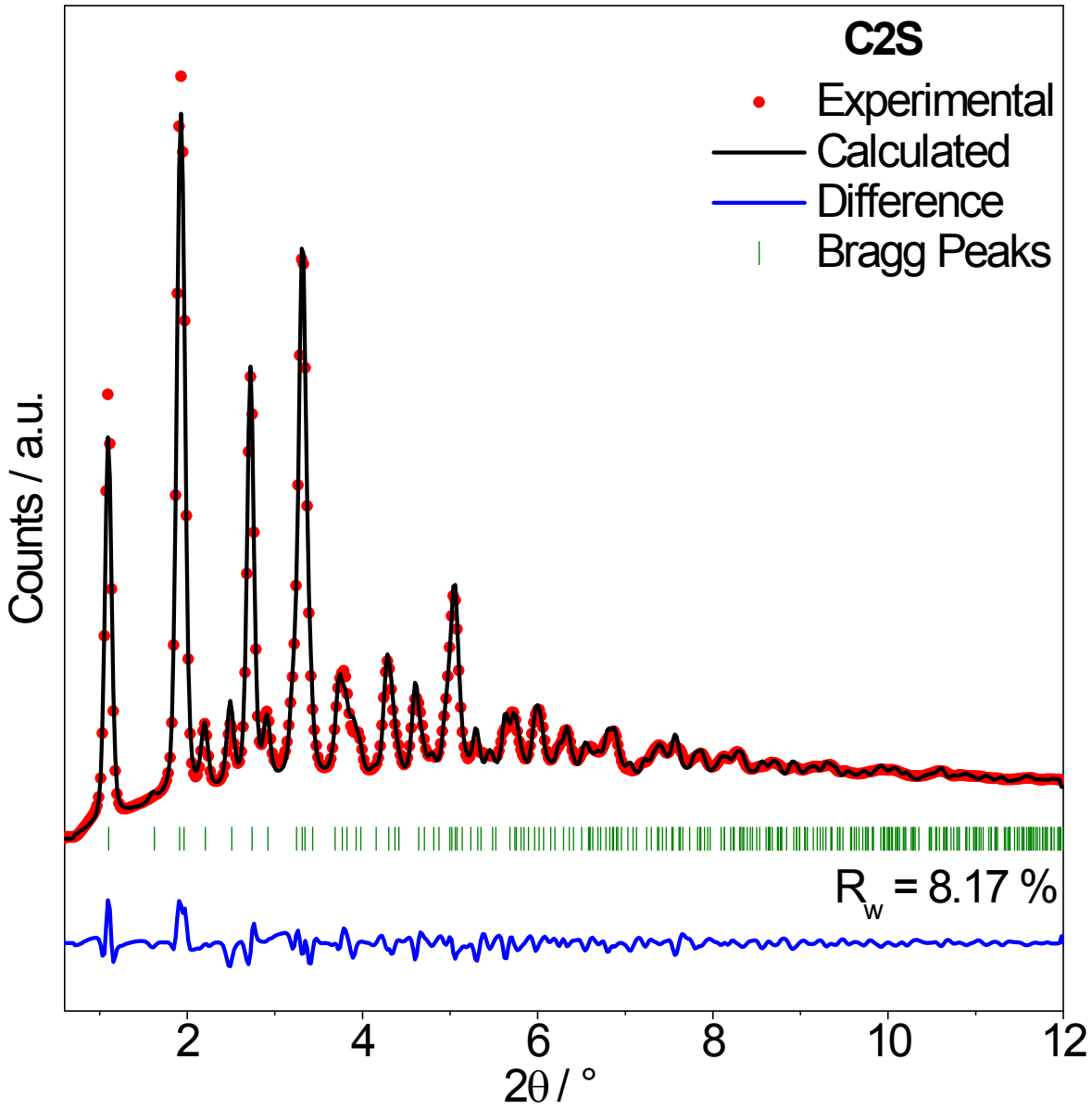

Figure S7. *Rietveld refinement of $NaEr_{0.8}Yb_{0.2}F_4$ / $NaYF_4$ / $NaGdF_4$ ($C2S_l$) upconverting nanocrystals based on a one-phase model. Red circles and black lines represent the experimental and calculated XPD patterns, respectively. The blue line (shifted for clarity) shows the difference between experimental and calculated XPD patterns. Bragg peaks positions are indicated by green tick marks. The goodness of fit (R_W value) is indicated (bottom right).*

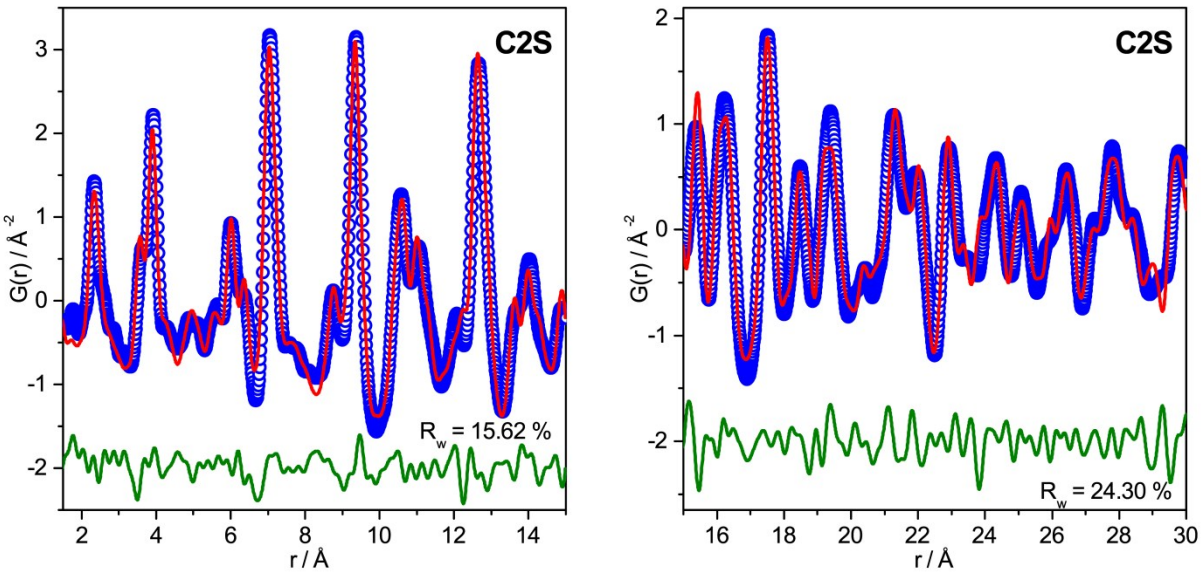

Figure S8. *PDF refinement of $NaEr_{0.8}Yb_{0.2}F_4$ / $NaYF_4$ / $NaGdF_4$ ($C2S_l$) upconverting nanocrystals based on a one-phase model. Blue circles and red lines represent the experimental and calculated PDF, respectively. The green lines (shifted for clarity) show the difference between experimental and calculated PDFs. PDF refinements were performed for the short- (left) and long- (right) r-ranges. The goodness of fit (R_W value) is indicated (bottom right).*

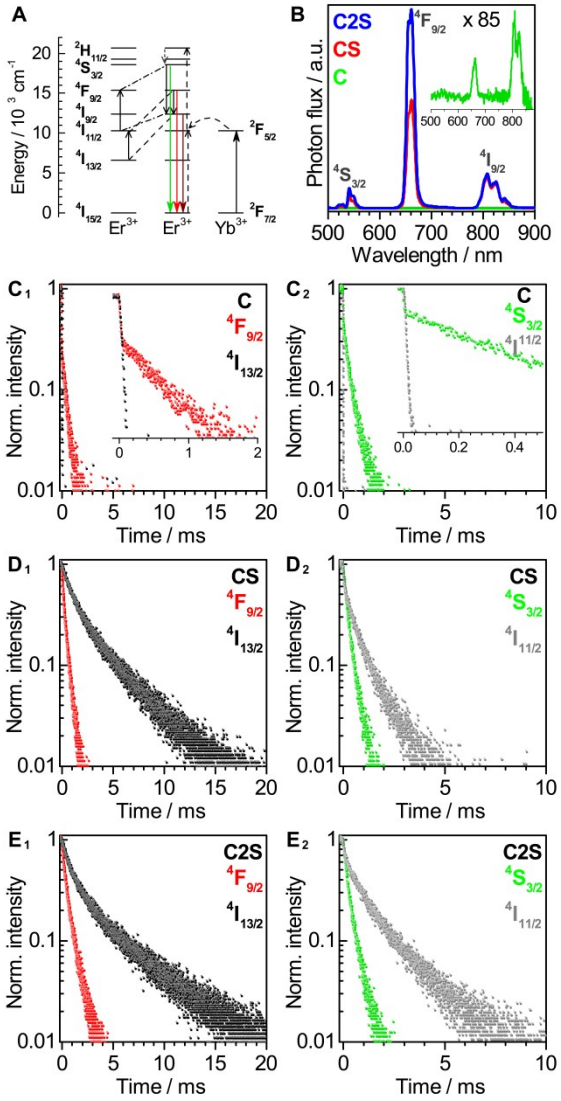

Figure S9. *(A) Partial electronic energy level diagram for Er^{3+} and Yb^{3+} with energy transfer mechanisms and upconversion emission under 980 nm excitation. (B) Upconversion emission spectra ($\lambda_{ex.}$ = 980 nm) of $NaEr_{0.8}Yb_{0.2}F_4$ (C, green), $NaEr_{0.8}Yb_{0.2}F_4/NaYF_4$ (CS_l, red), and $NaEr_{0.8}Yb_{0.2}F_4/NaYF_4/NaGdF_4$ ($C2S_l$, blue) nanocrystals (NCs). (C_1-E_1) Time-dependent photoluminescence measurements of the 1522 nm (black) and 656 nm (red) excited states of the C (C_1), CS (D_1), and C2S (E_1) NCs. (C_2-E_2) Time-dependent photoluminescence measurements of the 990 nm (gray) and 542 nm (green) excited states of the C (C_2), CS (D_2), and C2S (E_2) NCs.*

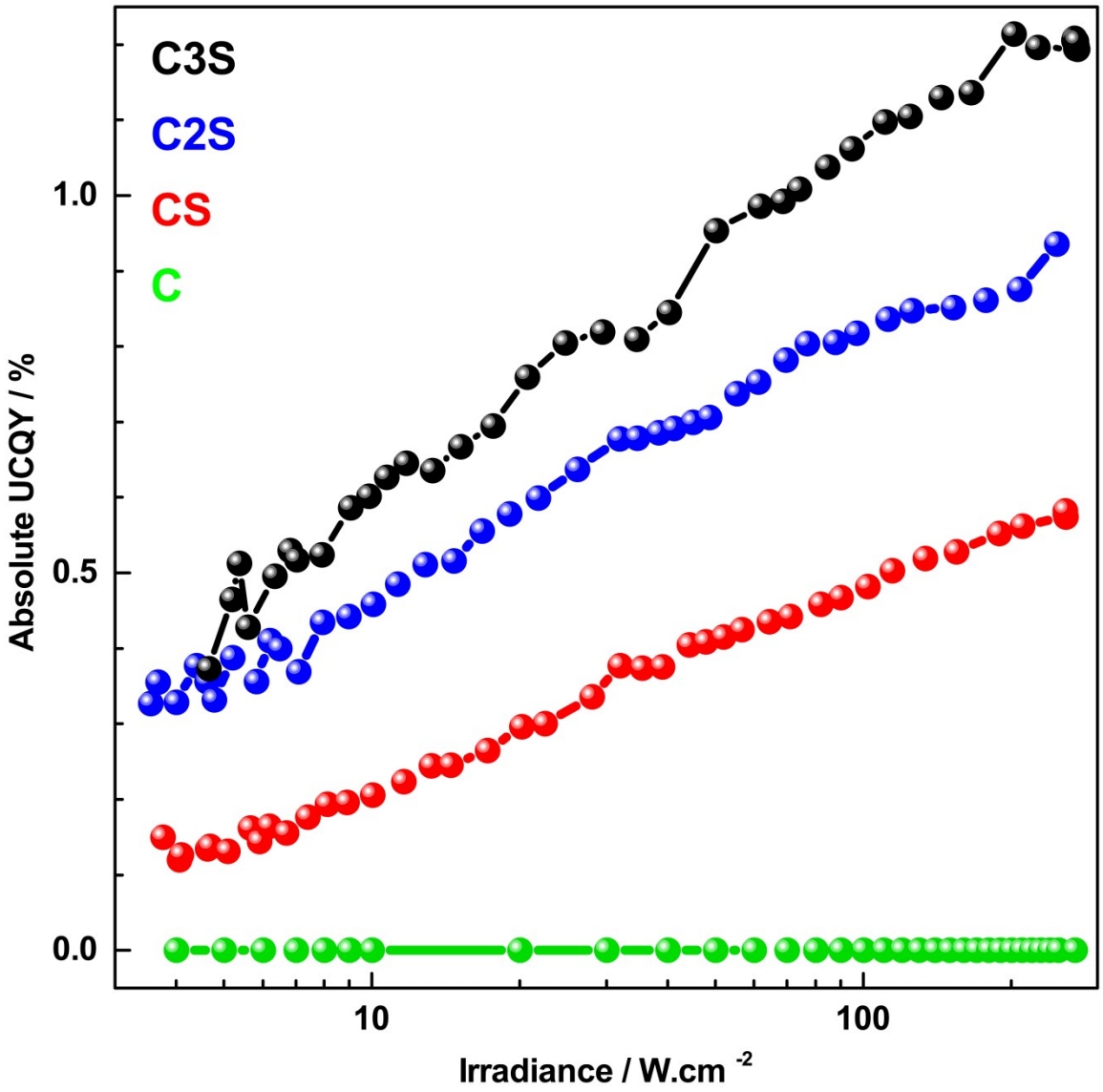

Figure S10. *Power-dependent absolute upconversion quantum yield ($\lambda_{ex.}$ = 980 nm) of $NaEr_{0.8}Yb_{0.2}F_4$ core (green), $NaEr_{0.8}Yb_{0.2}F_4/NaYF_4$ CS (red), $NaEr_{0.8}Yb_{0.2}F_4/NaYF_4/NaGdF_4$ C2S (blue), and $NaEr_{0.8}Yb_{0.2}F_4/NaYF_4/NaGdF_4/NaYF_4$ C3S upconverting nanocrystals (NCs). All single- and multi-shell NCs were synthesized with the same shell deposition method, namely Method I.*

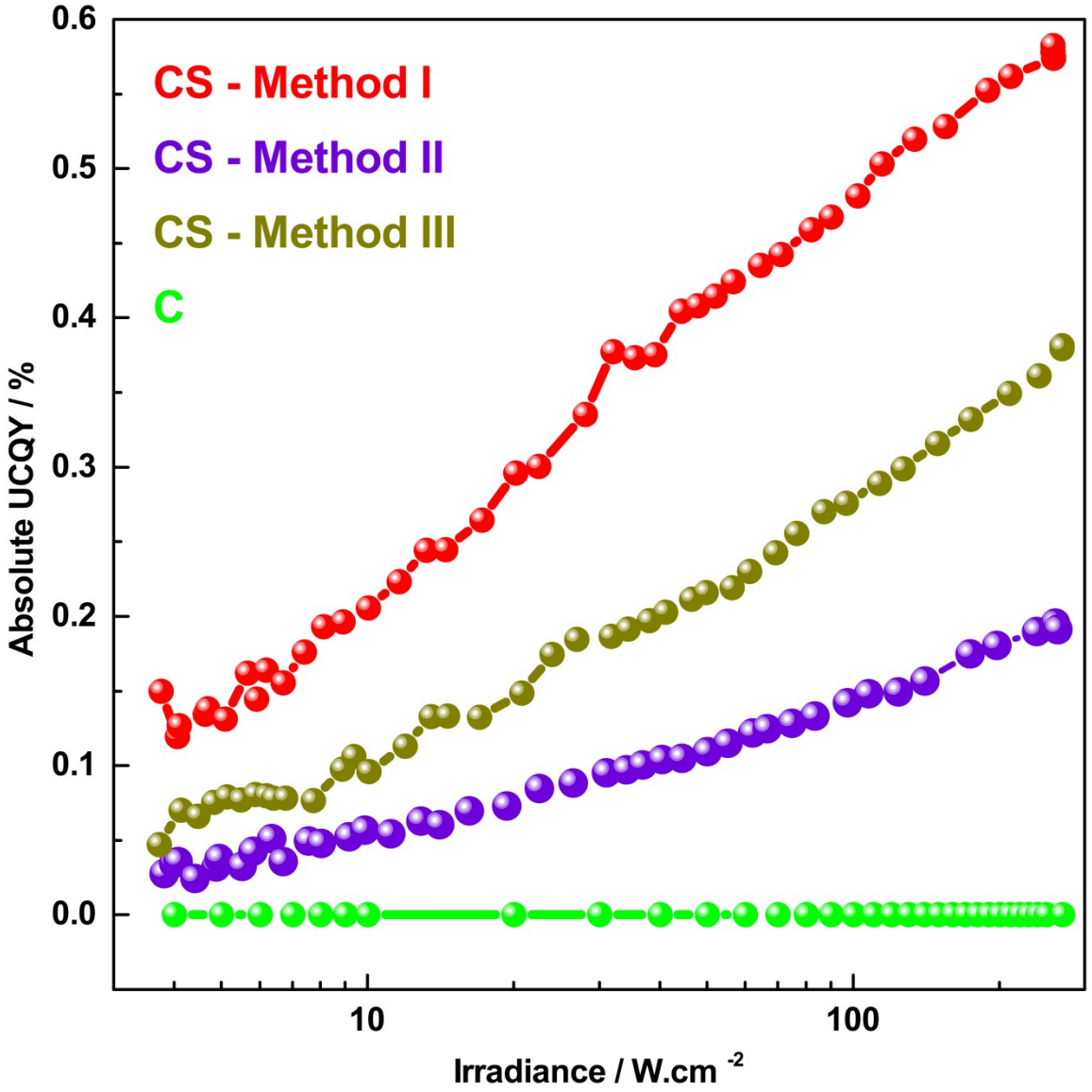

Figure S11. *Power-dependent absolute upconversion quantum yield ($\lambda_{ex.}$ = 980 nm) of $NaEr_{0.8}Yb_{0.2}F_4$ core (green) upconverting nanocrystals (NCs) compared to $NaEr_{0.8}Yb_{0.2}F_4/NaYF_4$ CS upconverting NCs synthesized with different shell deposition methods: Method I (red), Method II (purple), and Method III (dark yellow).*

10. Discussion regarding the optical properties

Energy levels of Er^{3+} and Yb^{3+} ions along with absorption, emission, and cross-relaxation mechanisms are schematically illustrated in Figure S9A. UC emission spectra of the different NCs weighted by their absorption are given in Figure S9B. The upconversion quantum yield (UCQY, Figures S10-S11) of the CS (0.57 % at 250 W/cm^2) is drastically higher than the C (10^{-4} % at 250 W/cm^2), while the UCQY of the C2S increases further (0.93 % at 250 W/cm^2). From the emission spectra, it is also obvious that the ratio of the $^4I_{9/2}$ to the sum of the $^4F_{9/2}$ and $^4S_{3/2}$ levels decreases as the shells are added. Note that the $^4I_{9/2}$ level can be created by cross-relaxations involving depletion of the $^4F_{9/2}$ and $^4S_{3/2}$ levels. When Er^{3+} is highly-concentrated, these cross-relaxations efficiently remove the visible UC and shift energy down to the near infrared. Lifetime measurements reveal two key pieces of information regarding the as-prepared NCs.

Firstly, surface quenching of the low-energy Er^{3+} $^4I_{13/2}$ and $^4I_{11/2}$ states are very significant for the core (Figure S9C), being greatly reduced by the presence of the first shell and further reduced via the addition of the second shell. This can be seen in i) the increase in the $^4I_{13/2}$ lifetime (3.55 ms to 4.84 ms) after cross-relaxation involving the $^4F_{9/2}$ can no longer take place and ii) the increase in the $^4I_{11/2}$ lifetime (1.24 ms to 1.88 ms) after cross relaxation involving the $^4S_{3/2}$ can no longer take place, as indicated in Figures S9D and S9E. This effect is expected because the increasing shell thickness decreases the chance of energy transfer to the surface of upconverting NCs preventing solvent quenching. However, the change in lifetime between the CS and C2S NCs clearly shows that pathways to the surface still exist after the first shell deposition, consistent with the formation of an intermixed region during shell deposition.

The second key piece of evidence from the lifetime analysis reveals the decrease in the Er^{3+}-ion concentration as both the first and second inert shells are deposited. In Figure S9C$_1$, the inset clearly illustrates how initially, when both the $^4I_{13/2}$ and $^4F_{9/2}$ states are populated, the decay of the $^4F_{9/2}$ population exactly matches that of the $^4I_{13/2}$ state. However, once the $^4I_{13/2}$ state is completely depleted (in this case by efficient surface quenching) the $^4F_{9/2}$ state decays with a much slower rate. This indicates that there is a very efficient cross relaxation that depopulates the $^4F_{9/2}$ state when an excited-state population in the $^4I_{13/2}$ level exists. As the shells are added the lifetime of the $^4I_{13/2}$ state is greatly enhanced, meaning that cross-relaxation occur over the entire $^4F_{9/2}$ state lifetime, and no switch to a longer-lifetime at late times occurs as in the core only. However, the $^4F_{9/2}$ state lifetime increases from the CS to the C2S NCs indicating that cross relaxation is decreased (despite the increase in the $^4I_{13/2}$ lifetime) by the addition of the second shell (Figures S9D$_1$-E$_1$). This decrease in cross-relaxation is then clear evidence that the concentration of the Er^{3+} ions has decreased due to the addition of the second Gd-based shell. An analogous argument can be made from the $^4I_{9/2}$ and $^4S_{3/2}$ lifetimes shown in Figures S9C$_2$-E$_2$.

A careful consideration of NCs optical properties reveals energy migration pathways to the surface and changes in the Er^{3+} concentration fully consistent with the chemical mapping and solid solution models. This strongly supports our conclusion that significant intermixing occurs during shell formation of large multi-shell architectures. Such an effect is not limited to ultra-small NCs and is important to consider for the comprehensive understanding of the structure-property relationships of multi-shell upconverting NCs.

11. Supplementary tables

	C			CS		
	Rietveld	PDF		Rietveld	PDF	
		1.5-15 Å	15-30 Å		1.5-15 Å	15-30 Å
Rw(%)	6.17	12.51	8 .29	6.24	14.08	9.7
Composition	$Na_{0.96(1)}(Er/Yb)_{1.04(1)}F_4$	Na (Er/Yb) F_4 (fixed)		$Na_{0.95(1)}$ $(Er/Yb)_{0.53(1)}$ $Y_{0.52(1)}F_4$	Na $(Er/Yb)_{0.5}$ $Y_{0.5}$ F_4 (fixed)	
a (Å)	5.963(1)	5.963	5.963(3)	5.9675(8)	5.967	5.967(2)
c (Å)	3.5066(8)	3.504	3.504(3)	3.5057(7)	3.503	3.503(2)
a/c	1.7005	1.7019	1.7019	1.7022	1.7035	1.7035
V ($Å^3$)	107.982	107.916	107.916	108.115	108.019	108.019
U_{iso}, RE1 ($Å^2$)	0.0050(6)	0.005(1)	0.005(2)	0.0052(6)	0.0043(9)	0.005(2)
U_{iso}, RE2/Na1 ($Å^2$)	0.0045(6)	0.005(3)	0.006(4)	0.0060(5)	0.005(2)	0.0044(39)
U_{iso}, Na2 ($Å^2$)	0.0055(6)	0.01(1)	0.01(1)	0.0101(6)	0.015(10)	0.013(11)
U_{iso}, F ($Å^2$)	0.0099(6)	0.026(9)	0.02(1)	0.0101(6)	0.026(6)	0.023(7(
Coherent length (nm)	15.84(3)	13.9	13.9(9.2)	23.79(3)	15.7	15.7(9.0)

Table S1. *Refined parameters from the Rietveld and PDF refinements of $NaEr_{0.8}Yb_{0.2}F_4$ (C_l), and $NaEr_{0.8}Yb_{0.2}F_4/NaYF_4$ (CS_l) upconverting nanocrystals based on a one-phase model.*

	C2S					
	Rietveld		PDF			
			1.5-15 Å		15-30 Å	
Rw(%)	5.97		12.50		8.03	
	Phase 1	Phase 2	Phase 1	Phase 2	Phase 1	Phase 2
Composition	$Na\ (Er/Yb)_{0.5}\ Y_{0.5}\ F_4$	$NaGdF_4$	$Na\ (Er/Yb)_{0.5}\ Y_{0.5}\ F_4$	$NaGdF_4$	$Na\ (Er/Yb)_{0.5}\ Y_{0.5}\ F_4$	$NaGdF_4$
Volume %	21(2)	79(4)	37(6)	63(6)	38(13)	62(13)
a (Å)	5.991(2)	6.036(1)	5.9953	6.03788	5.995(9)	6.038)9)
c (Å)	3.527(2)	3.583(1)	3.511	3.57703333	3.511(8)	3.577(7)
a/c	1.6988	1.6844	1.7074	1.6879	1.704	1.6879
V ($Å^3$)	109.641	113.042	109.302	112.933	109.30	112.9334
U_{iso}, RE1 ($Å^2$)	0.007(2)	0.006(1)	0.003(1)	0.006(3)	0.006(4)	0.008(3)
U_{iso}, RE2/Na1 ($Å^2$)	0.007(2)	0.007(1)	0.008(4)	0.0049(45)	0.008(1)	0.010(7)
U_{iso}, Na2 ($Å^2$)	0.009(2)	0.006(1)	0.03(2)	0.019(8)	0.02(2)	0.03(2)
U_{iso}, F ($Å^2$)	0.009(2)	0.006(1)	0.03(2)	0.019(8)	0.02(2)	0.02(1)
Coherent length (Å)	24.40(1)	15.87(6)	35.8	9.5	35.8(1.8)	9.5(5.7)

Table S2. *Refined parameters from the Rietveld and PDF refinements of* $NaEr_{0.8}Yb_{0.2}F_4 | NaYF_4 | NaGdF_4$ ($C2S_I$) *upconverting nanocrystals based on a two-phase model.*

12. References

[1] Nanotechnology **2008**, 19, 345606.

[2] Nature Protocols **2014**, 9, 1634.

[3] Journal of the American Chemical Society **2006**, 128, 6426.

[4] http://www.jems-saas.ch

[5] RSC Advances **2012**, 2, 9473.

[6] High Pressure Research **1996**, 14, 235.

[7] Physica B Condensed Matter. **1993**, 192, 55.

[8] Journal of Applied Crystallography **2013**, 46, 560.

[9] Journal of Physics: Condensed Matter **2007**, 19, 335219.